Ductility of bulk metallic glass composites: Microstructural effects

F. Abdeljawad,[1] M. Fontus,[2] and M. Haataja[1,3,4,a)]
[1]*Department of Mechanical and Aerospace Engineering, Princeton University, Princeton, New Jersey 08544, USA*
[2]*Undergraduate Medical Academy, Prairie View A&M University, Prairie View, Texas 77446, USA*
[3]*Princeton Institute for the Science and Technology of Materials (PRISM), Princeton University, Princeton, New Jersey 08544, USA*
[4]*Program in Applied and Computational Mathematics (PACM), Princeton University, Princeton, New Jersey 08544, USA*

(Received 1 November 2010; accepted 2 December 2010; published online 21 January 2011)

Recent experimental findings suggest that the problem of catastrophic failure by shear band propagation in monolithic bulk metallic glasses (BMGs) can be mitigated by forming two-phase composites consisting of a glassy metal matrix phase and a soft crystalline reinforcement phase. Here, we employ a recently introduced phase-field model in two spatial dimensions, capable of capturing shear banding in BMG systems, to address the effects of microstructure on the mechanical properties of BMG composites. We identify an important geometric length scale associated with the dendritic particles and demonstrate that it controls the overall ductility and ultimate strength of such BMG composites. © *2011 American Institute of Physics*. [doi:10.1063/1.3531660]

Monolithic bulk metallic glasses (BMGs) are characterized by their near theoretical strength and large elasticity limit.[1,2] On the other hand, monolithic BMGs exhibit limited amount of global plasticity prior to catastrophic failure via the propagation of highly localized shear bands.[2] Recently, a new class of composite metallic systems has emerged, where the amorphous metal constitutes the matrix phase and soft crystalline dendrites form the reinforcement phase.[3,4] Experiments suggest that the problem of catastrophic failure by highly localized shear banding in monolithic BMGs can be mitigated by introducing such two-phase microstructures, wherein ductile crystalline dendrites can promote strain localization at multiple sites throughout the sample and act as microstructural arrest barriers to shear band propagation. The result is a stable BMG composite against catastrophic single shear band propagation.[5–7] While it has been recently suggested that ductility, tensile, and fatigue strengths of BMG composites can be enhanced by tailoring the microstructural length scales of the crystalline domains (characterized by the primary and secondary dendrite arms),[6,8] the roles of reinforcement size and morphology on the deformation patterns of these composites have not been fully explored.

In this letter, we employ the diffuse-interface approach introduced recently by Abdeljawad and Haataja[9] to investigate the size and morphology-dependent mechanical properties of BMG composites under simple shear. We demonstrate that in addition to the area fraction of the ductile phase, tailoring the spatial length scales associated with the dendrites plays a key role in the deformation behavior and mechanical properties of BMG composites.

Traditionally, the focus of theoretical work has been on either atomistic properties of BMG composites, which are difficult to scale up,[10,11] or mesoscale descriptions of strain localization in monolithic BMGs, which incorporate shear transformation zones (STZs) as the main carrier of plasticity in mean-field theory.[12,13] In contrast, the phase-field approach from Ref. 9 naturally accounts for the presence of structural heterogeneities at a coarse-grained level in the glassy phase, the presence of ductile particles, and the formation and propagation of shear bands, which at the atomic level result from the sequential triggering of local STZs. In this model, strain localization via shear banding is modeled as a phase transition between "unslipped" and "slipped" states.

Within the diffuse-interface formalism and in two dimensions, a nonlinear form for the deformation energy of a BMG system is written in terms of the spatial derivatives of the displacement field $\mathbf{u}(\mathbf{r},t)$ as[9]

$$\mathcal{F}=\int d\mathbf{r}\left[\frac{K(\mathbf{r})}{2}(u_{xx}+u_{yy})^2+\frac{\mu(\mathbf{r})}{2}\left((u_{xx}-u_{yy})^2+\frac{\Delta^2(\mathbf{r})}{2\pi^2}\left\{1-\cos\left[\frac{2\pi}{\Delta(\mathbf{r})}(u_{xy}+u_{yx})\right]\right\}\right)\right]+\frac{W^2}{2}\int d\mathbf{r}[(\nabla u_{xx})^2+(\nabla u_{yy})^2+4(\nabla\epsilon_{xy})^2], \quad (1)$$

where $u_{ij}\equiv\partial u_i/\partial x_j$ and $\epsilon_{ij}\equiv 1/2(u_{ij}+u_{ji})$. $K(\mathbf{r})$ and $\mu(\mathbf{r})$ denote the bulk and shear moduli, respectively, while $\Delta(\mathbf{r})$ sets the local shear strain and controls the energy barrier associated with slip events. In the crystalline phase, $\Delta(\mathbf{r})$ is constant,[14] while in the glassy phase, structural heterogeneity is incorporated by treating $\Delta(\mathbf{r})$ as a quenched, Gaussian random variable[15] with average $\langle\Delta(\mathbf{r})\rangle=\Delta_0$ and a two-point correlation function $\langle[\Delta(\mathbf{r})-\Delta_0][\Delta(\mathbf{r}')-\Delta_0]\rangle=\sigma^2\exp(-|\mathbf{r}-\mathbf{r}'|/\xi)$, where σ^2 and $\xi\sim 5$ nm denote the variance of the distribution and a structural correlation length corresponding to the STZ size, respectively. As usual in phase-field approaches, the last term in Eq. (1) contains higher order gradients in the displacement field which, phenomenologically, suppress strain gradients on scales $\lesssim W/\sqrt{\mu}$, where W is an effective interfacial energy. Finally, the dynamics of the dimensionless displacement field follow from

a)Electronic mail: mhaataja@princeton.edu.

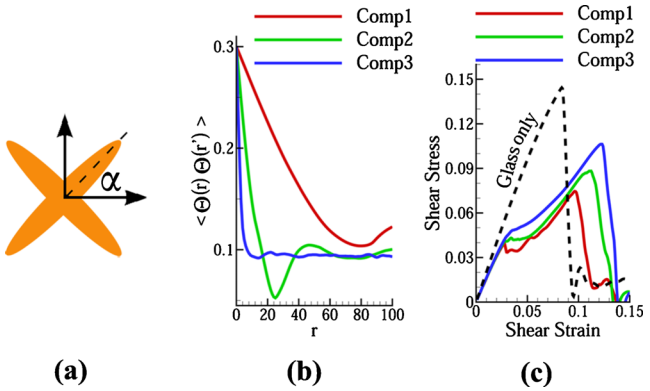

FIG. 1. (Color online) (a) Idealization of a crystalline dendrite in a BMG composite. α is the random orientation angle of the dendrite. (b) Two-point correlation function. (c) Shear stress-strain curves for the BMG composites, Comp1, Comp2, and Comp3, with 30% area faction of the ductile phase.

$$\frac{\partial^2 u_i}{\partial t^2} - \eta^* \nabla^2 \frac{\partial u_i}{\partial t} = -\Gamma^* \frac{\delta F}{\delta u_i}, \quad i = x, y, \tag{2}$$

where Γ^* and η^* are dimensionless parameters controlling the elastic wave speed and the damping characteristics of the system, respectively. Spatial dimensions and stresses were expressed in terms of the structural correlation length, and the shear modulus of the ductile phase, respectively. BMG systems were simulated under simple shear with a net macroscopic strain of 18%. The dynamical equations for the displacement field were integrated on a 512×512 uniform lattice with $\Delta x = \Delta y = 1.0$ and a time step $\Delta t = 0.003$. $\eta^* = 80$ and $\Gamma^* = 240$ were chosen such that stresses relax effectively instantaneously relative to the externally imposed (dimensionless) strain rate, 2×10^{-4}. To simulate simple shear, the top edge of the simulation box was displaced relative to the bottom edge at the prescribed strain rate, while periodic boundary conditions were employed lengthwise.

In order to investigate the role of microstructure on the mechanical behavior of BMG composites, we model each dendrite as two perpendicularly intersecting ellipses, shown in Fig. 1(a), with the angle α representing the orientation of the dendrite. We note that the proposed dendrite morphology collapses to the case of circular disks studied in Ref. 9 when the major and minor axes (L_a and L_b, respectively) of the intersecting ellipses are set equal. Realizations of BMG composite microstructures were generated by randomly placing the ductile dendrites with random orientations in the glassy matrix. Here, the design parameters are the total area fraction of the crystalline phase ϕ and the length scales L_a and L_b associated with the dendrites. In order to extract a characteristic length scale D for the crystalline dendrites, the two-point correlation function $G(r) = \langle \Theta(\mathbf{R}) \Theta(\mathbf{R}+\mathbf{r}) \rangle$ for the BMG composite was calculated, where $\Theta(\mathbf{r})$ is a local phase indicator with $\Theta(\mathbf{r}) = 1.0$ in the dendritic phase and zero elsewhere. More specifically, $D \sim (L_a L_b)^{1/2}$ corresponds to the point of the first minimum in $G(r)$. Furthermore, $K(\mathbf{r}) = 2.17$, $\mu(\mathbf{r}) = 1.0$, and $\Delta(\mathbf{r}) = 0.2$ in the crystalline phase, and 4.33, 2.0, and Δ_0 in the glass, where Δ_0 was set such that $\langle \Delta(\mathbf{r}) \rangle_{\mathrm{BMG}}$ for the BMG composite is kept at 0.6. Thus, $\Delta_0 = (\langle \Delta(\mathbf{r}) \rangle_{\mathrm{BMG}} - \phi \Delta(\mathbf{r})_{\mathrm{crystal}}) / (1 - \phi)$. Finally, $\sigma^2 = 0.005$, $\xi = 2.5$, and $W = 1.0$.

We begin our exploration of the model by examining the effects of dendrite morphology and the associated length scales on the deformation patterns of BMG composites. To this end, three BMG composites, Comp1, Comp2, and Comp3, each with $\phi = 0.3$ and $\Delta_0 = 0.771$ but differing in the characteristic length scales associated with the dendritic microstructure, were examined. Figure 1(b) displays $G(r)$ for Comp1, Comp2, and Comp3, for which $D \approx 82$, 25, and 14, respectively. Figures 2(a)–2(c) in turn show representative microstructures of Comp1, Comp2, and Comp3. In Comp1, dendrites are represented by monodispersed disks whereas in Comp2, the more ramified dendrites form spatially disconnected regions. Finally, in Comp3, the dendrites are highly stretched ellipses that form a connected framework. Contours of shear strain at 10% nominal strain are shown in Figs. 2(d)–2(f) for Comp1, Comp2, and Comp3, respectively. The nonuniform strain distribution is due to the heterogeneous nature of the microstructures. In Comp1, a shear band formed and started to extend throughout the sample while in Comp2, pockets of localized strain can be seen. Strain is more globally distributed in Comp3 with no signs of shear banding. Figures 2(g)–2(i) show strain contours at 11.5% nominal strain for Comp1, Comp2, and Comp3, respectively. A fully developed shear band can be seen in Comp1 while in Comp2, several shear bands started to form and propagate in the sample implying extensive plasticity prior to catastrophic failure. In Comp3, strain is still globally distributed with the appearance of pockets of localized strain. To quantify the instance of shear banding, we examined shear stress-strain curves for these composites, shown in Fig. 1(c). In all composite systems, local slip events occur at ~3% nominal strain but the composites continue to strain harden until the ultimate strength is reached. The BMG composite with smaller dendrites, Comp3, exhibits more ductility (total strain to failure) and a higher strength value than the ones with larger dendrites, Comp1 and Comp2. Nominal strains at

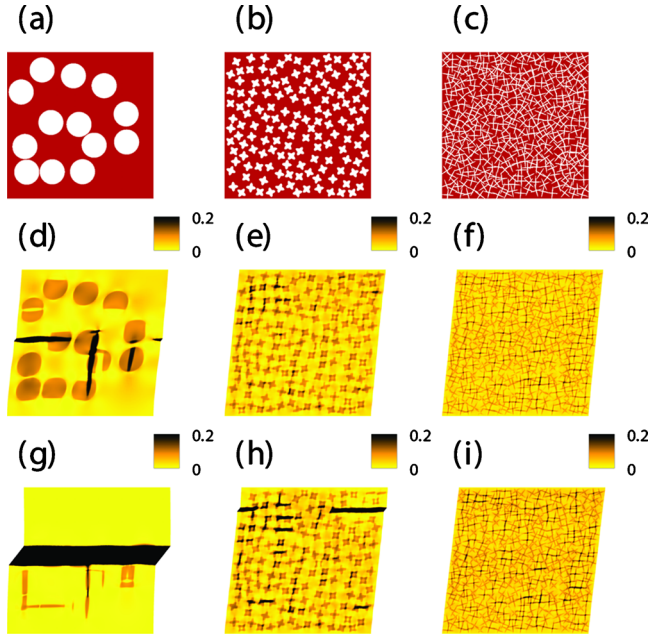

FIG. 2. (Color online) Representative BMG composite microstructures for (a) Comp1, (b) Comp2, and (c) Comp3. Dark (light) domains represent glassy (ductile) phase. Shear strain contours at 10% nominal strain for (d) Comp1, (e) Comp2, and (f) Comp3. Shear strain contours at 11.5% nominal strain for (g) Comp1, (h) Comp2, and (i) Comp3.

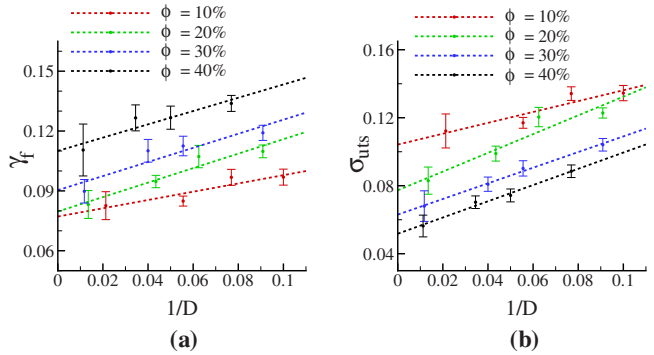

FIG. 3. (Color online) (a) Total strain to failure γ_f and (b) ultimate strength σ_{uts} for BMG composites as a function of $1/D$ at different ϕ values, where D is the characteristic length scale associated with the dendritic phase and ϕ is the area fraction of the ductile phase.

the onset of shear banding are ~9%, 11%, and 13% for Comp1, Comp2, and Comp3, respectively.

Next we quantify the microstructural effects by examining the total strain to failure γ_f and ultimate strength σ_{uts} as a function of both the area fraction ϕ and the characteristic length scale D associated with the dendritic particles. We simulated BMG composites with ϕ ranging from 10% to 40%. For a given ϕ, several realizations of BMG composites were obtained spanning multiple length scales for the crystal domain size. To account for sample-to-sample variations, results were averaged over ten runs. Figures 3(a) and 3(b) show plots of γ_f and σ_{uts}, respectively, as a function of $1/D$. The results suggest that γ_f and σ_{uts} scale with $1/D \sim (L_a L_b)^{-1/2}$, implying that, at a fixed ϕ, ductility and strength can be enhanced by tailoring the length scales associated with the dendritic particles. More specifically, for a fixed ϕ, BMG composites with fine-scale microstructural features exhibit better mechanical properties than the ones with coarser crystal domains. In particular, these results suggest that for dendritic morphologies, the relevant length scale for the overall mechanical properties of the composites is $(L_a L_b)^{1/2}$, that is, the geometric mean of the dendrite arm length and width.

In summary, the model introduced in Ref. 9 was employed to examine the effects of BMG composite microstructures, characterized by the area fraction and the characteristic length scale associated with the ductile dendritic phase, on the mechanical properties of such composites. Our results suggest that in addition to the area fraction of the ductile phase, tailoring the spatial length scales associated with the dendrites plays a key role in the deformation behavior and mechanical properties of BMG composites. Perhaps most importantly, these results suggest that for dendritic morphologies, the relevant length scale for mechanical properties of such composites is $(L_a L_b)^{1/2}$, that is, the geometric mean of the dendrite arm length and width.

This work has been in part supported by an NSF-DMR Grant No. DMR-0449184 (M.H.), NSF-DMR Grant No. DMR-0819860 (M.H. and M.F.), and NSF-HRD Grant No. HRD-0917335 (M.F.). Useful discussions with Dr. Lisa Manning are gratefully acknowledged.

[1] A. L. Greer, Science **267**, 1947 (1995).
[2] A. R. Yavari, J. Lewandowski, and J. Eckert, MRS Bull. **32**, 635 (2007).
[3] H. Choi-Yim and W. L. Johnson, Appl. Phys. Lett. **71**, 3808 (1997).
[4] C. Fan, R. T. Ott, and T. C. Hufnagel, Appl. Phys. Lett. **81**, 1020 (2002).
[5] D. C. Hofmann, J.-Y. Suh, A. West, M.-L. Lind, M. D. Demetriou, and W. L. Johnson, Proc. Natl. Acad. Sci. U.S.A. **105**, 20136 (2008).
[6] D. C. Hofmann, J. Y. Suh, A. Wiest, G. Duan, M. L. Lind, M. D. Demetriou, and W. L. Johnson, Nature (London) **451**, 1085 (2008).
[7] M. L. Lee, Y. Li, and C. A. Schuh, Acta Mater. **52**, 4121 (2004).
[8] M. E. Launey, D. C. Hofmann, W. L. Johnson, and R. O. Ritchie, Proc. Natl. Acad. Sci. U.S.A. **106**, 4986 (2009).
[9] F. Abdeljawad and M. Haataja, Phys. Rev. Lett. **105**, 125503 (2010).
[10] A. C. Lund and C. A. Schuh, Philos. Mag. Lett. **87**, 603 (2007).
[11] Y. Shi and M. L. Falk, Acta Mater. **56**, 995 (2008).
[12] M. L. Falk and J. S. Langer, Phys. Rev. E **57**, 7192 (1998).
[13] E. Homer and C. A. Schuh, Acta Mater. **57**, 2823 (2009).
[14] A. Minami and A. Onuki, Acta Mater. **55**, 2375 (2007).
[15] At low temperatures (relative to the glass transition temperature), we expect that Δ remains "frozen" up until the propagation of shear bands. On the other hand, at elevated temperatures, a physically based description of Δ has to account for the emergence of deformation history-dependent disorder.